

Feedback Sensitivity and Coherence Collapse Threshold of Semiconductor DFB Lasers With Complex Structures

Frédéric Grillot, *Member, IEEE*, Bruno Thedrez, and Guang-Hua Duan, *Senior Member, IEEE*

Abstract—A general method for evaluating the feedback sensitivity of semiconductor lasers is proposed based on Green's functions approach. The rate equations derived in this paper generalize works already published to any type of laser cavities such as those with axially varying parameters. The variation of the lasing frequency occurring under external optical feedback is then used to predict the coherence collapse threshold. The approach is validated for conventional DFB lasers by comparing the calculated feedback sensitivity with those obtained from analytical expressions. Both feedback sensitivity and coherence collapse thresholds are then calculated and analyzed for DFB lasers with a chirped grating. A remarkable agreement on the critical feedback level between simulations and measurements is obtained for all the lasers under study.

Index Terms—DFB lasers, Green function, optical feedback, transfer function matrix.

I. INTRODUCTION

IT IS WELL KNOWN that the performances of a semiconductor laser are strongly altered by any source of external optical feedback. The laser sensitivity can be such that, even under a very weak feedback level, the laser becomes unstable and starts operating within the so-called coherence collapse regime [1]. The main consequence of such a regime on the semiconductor laser is a drastic broadening of the laser linewidth up to several gigahertz which is very detrimental to most applications. In the important case of optical fiber transmission, the coherence collapse leads to a strong degradation in the bit error rate (BER) when the laser is used as a transmitter, as theoretically [2] and experimentally [3] demonstrated. More generally, the prediction of the coherence collapse threshold is an important feature for all applications requiring either a low noise level or a proper control of the laser coherence.

Based on a weak coherent feedback hypothesis, the determination of the critical feedback threshold was analytically derived for Fabry-Perot lasers in [4]. An analytical method was also proposed by Favre to determine the feedback sensitivity, or the coupling strength coefficients, of DFB lasers [5]. Both approaches

concluded the importance of calculating the coupling strength coefficients of the laser cavity [6]. Following [5], the coherence collapse threshold of DFB lasers having an antireflection (AR) coating on the emission facet and a high-reflection (HR) coating on the rear facet has been calculated and compared to experimental results [7]. It was both theoretically and experimentally shown in [7] that, due to the HR-facet, the feedback sensitivity as well as the coherence collapse threshold exhibit a facet phase dependence through a quasi-parabolic distribution. The large dispersion among the critical feedback levels observed for a given set of DFB lasers leads to a wide range of behavior under external optical feedback which is detrimental to applications. However, the feedback sensitivity of chirped grating DFB lasers for which excellent performance uniformity has been reported [8] could not be assessed with the method described in [5] due to the complicated nature of the grating. The method in [5] therefore needs to be extended by a new approach that can provide a general method of calculation of the feedback sensitivity and of the coherence collapse valid for any type of laser. Developing and validating such an approach is the main goal of this paper.

The paper is organized as follows. In Section II, the Lang and Kobayashi rate equations describing a semiconductor laser operating under external optical feedback are generalized using Green's functions approach [9]. An expression of the variation of the lasing angular frequency serving for the calculation of both the feedback sensitivity and of the coherence collapse is then derived from our generalized dynamical equations. A very general expression of the feedback sensitivity valid for any laser cavity comes as a consequence of these equations. In Section III, the feedback sensitivity of DFB lasers is calculated by using this new method and compared to the Favre analytical method described in [5] to validate the new approach. In Section IV, chirped grating DFB lasers are investigated. After coupling strength coefficient calculations, the coherence collapse threshold is determined for several designs. A successful comparison between calculated and measured coherence collapse thresholds confirms the validity of the approach. Finally, we summarize our results and conclusions in Section V. Overall, the generalization of the Lang and Kobayashi equations allows us to demonstrate a new successful and powerful numerical tool serving to evaluate the feedback sensitivity and the coherence collapse threshold of semiconductor DFB lasers with complex structures.

Manuscript received July 22, 2003; revised November 14, 2003.

F. Grillot was with the OPTO+, Alcatel Research and Innovation, Route de Nozay, F-91460 Marcoussis, France. He is now with Institut d'Electronique Fondamentale, UMR CNRS 8622, Université de Paris-Sud, F-91405 Orsay Cedex, France (e-mail: frederic.grillot@ief.u-psud.fr).

B. Thedrez and G.-H. Duan are with the OPTO+, Alcatel Research and Innovation, Route de Nozay, F-91460 Marcoussis, France.

Digital Object Identifier 10.1109/JQE.2003.823031

II. GENERALIZED THEORY OF OPTICAL FEEDBACK

In this section, a new method of calculation of both the feedback sensitivity and the coherence collapse threshold is reported. This new method covers most type of laser structures at and above threshold. In particular, longitudinal variations along the laser axis as well as spatial hole burning effects [10] are included.

A. Generalized Rate Equations Including External Optical Feedback

In what follows, it is assumed that the cavity medium is isotropic and the laser perfectly index-guided. In addition to these conditions, the longitudinal axis only is explicitly taken into account. Both transverse and lateral variations are accounted for by the effective dielectric constant ε . The starting point is the wave equation for the electromagnetic field. From Maxwell's equations under the previous assumptions, the complex Fourier component $E_\omega(z)$ of the electric field in the laser cavity is governed by the one-dimensional (1-D) scalar wave equation [9], [12], [13]

$$\nabla_z^2 E_\omega(z) + k_0^2 \varepsilon E_\omega(z) = F_\omega(z). \quad (1)$$

In (1), $\nabla_z^2 = \partial^2/\partial z^2$ is the Laplacian operator for the longitudinal coordinate z , $\omega/2\pi$ is the lasing frequency, $k_0 = \omega/c$ is the wavenumber, where c is the velocity of light in vacuum, ε is the complex dielectric constant, and $F_\omega(z)$ is the frequential Langevin force term accounting for the distributed spontaneous emission. It has been shown that the propagation wave equation can be solved by using Green's functions theory and that the general solution of (1) can be written through the integral relation [9], [12], [13]

$$E_\omega(z) = \int_{(L)} G_\omega(z, z') F_\omega(z') dz'. \quad (2)$$

In (2), the integration is done over the total laser cavity length L and includes the Green's function $G_\omega(z, z')$ whose expression is given by [9]

$$G_\omega(z, z') = \frac{Z_+(z_>)Z_-(z_<)}{W(\omega, N(z), \rho_k)} \quad (3)$$

where $z_<$ and $z_>$ correspond to the lesser or greater values of z and z' , $Z_+(z)$ and $Z_-(z)$ are two independent solutions of the homogeneous part of (1) with respect to the boundary conditions, respectively, on the left and right facets. Finally, it is important to point out that, in (3), $W(\omega, N(z), \rho_k)$ is the Wronskian term of the previous solutions depending on the lasing frequency $\omega/2\pi$, the carrier density $N(z)$, and the amplitude reflectivity ρ_k of the k -facet (with $k = r$ for the right facet and $k = l$ for the left facet). The dependence of the Wronskian on the facet reflectivity will be used later to take into account external optical feedback coming from a distant reflecting point of amplitude reflectivity $\gamma \ll 1$. By injecting (3) into (2), the general solution giving the electric field in the laser cavity becomes

$$E_\omega(z) = \int_{(L)} \frac{Z_+(z_>)Z_-(z_<)}{W(\omega, N(z), \rho_k)} F_\omega(z') dz'. \quad (4)$$

It is well known that the oscillation condition corresponds to a zero in the Wronskian term which serves to determine the laser longitudinal mode. Such a condition can be written as follows:

$$W(\omega_0, N_0(z), \rho_k) = 0. \quad (5)$$

As the Wronskian is complex, both the lasing frequency $\omega_0/2\pi$ and the carrier density distribution at threshold N_0 are completely determined from (5). Assuming that the semiconductor laser operates only in one longitudinal mode, the field distribution can be simplified and is denoted by $Z_+(z) = Z_-(z) = Z_0(z)$. When the laser is exposed to external feedback, the lasing frequency and the carrier density distribution deviates from their original values. As a result, the new Wronskian describing the lasing conditions under feedback can be developed as [13], [14]

$$W(\omega, N(z), \rho_{k,eq}) = W(\omega_0, N_0(z), \rho_k) + \frac{\partial W}{\partial \omega} \Delta \omega + \frac{1}{L} \int_{(L)} \frac{\partial W}{\partial N} \Delta N dz + \frac{\partial W}{\partial \rho_k} \Delta \rho_k \quad (6)$$

where $\Delta \omega = \omega - \omega_0$, $\Delta N = N - N_0$, and $\Delta \rho_k = \rho_{k,eq} - \rho_k$ is the variation of the k -facet reflectivity induced by external optical feedback [5], [15] as follows:

$$\Delta \rho_k = (1 - \rho_k^2) \gamma e^{-j\omega\tau}. \quad (7)$$

In (7), $\omega/2\pi$ is the lasing frequency in the presence of optical feedback and $\tau = 2L_e/c$ is the external round-trip time (where L_e is the external cavity length and c is the velocity of light in vacuum). As was mentioned at the beginning of this section, spatial hole burning effects are also taken into account in (6) through the integral term over the cavity length. By multiplying the two sides of (4) by $jW(\omega, N(z), \rho_k)/Z_0(z)$ and using (6), the rate equation for the electric field is thus obtained after the inverse Fourier transform of (4), [9], [13] as follows:

$$\frac{d\xi_0(t)}{dt} = \left[j(\omega_0 - \omega) - \frac{j}{L} \int_{(L)} \frac{\partial W/\partial N}{\partial W/\partial \omega} \Delta N dz \right] \xi_0(t) - j \frac{\partial W/\partial \rho_k}{\partial W/\partial \omega} \gamma (1 - \rho_k^2) \xi_0(t - \tau) + F(t) \quad (8)$$

where $\xi_0(t)$ represents the slowly varying envelope of the electrical field in the laser cavity

$$\xi_0(t) = \frac{1}{2\pi} \int_{-\infty}^{+\infty} \xi_\omega e^{j\omega t} d\omega \quad (9)$$

where $\xi_\omega = E_\omega/Z_0(z)$, and $F(t)$ is the Langevin force in the time domain. It is important to note that (8) can be applied to any type of semiconductor lasers. The third term of (8) extends the known Green's function approach [12], [13] to the case of external optical feedback and constitutes a generalization of the Lang and Kobayashi rate equations. To convert the field complex amplitude rate equation into photon density P and phase ϕ rate equations, let us write the complex electrical field as

$$\xi_0(t) = \sqrt{P(t)} e^{j\phi(t)} \quad (10)$$

where $P(t)$ is the photon number inside the cavity and ϕ is the phase of the electrical field. By injecting (10) into (8) and after

having separated the real and imaginary parts, the dynamic evolution of the electric field of a semiconductor laser operating under external optical feedback is given by

$$\frac{dP}{dt} = \frac{2}{L} \int_{(L)} W_{N_i} \Delta N dz P + 2Im \left[W_p \gamma (1 - \rho_k^2) \frac{\xi_0(t - \tau)}{\xi_0(t)} \right] P + F_p(t) \quad (11)$$

$$\frac{d\phi}{dt} = \omega_0 - \omega - \frac{1}{L} \int_{(L)} W_{N_r} \Delta N dz - Re \left[W_p \gamma (1 - \rho_k^2) \frac{\xi_0(t - \tau)}{\xi_0(t)} \right] + F\phi(t) \quad (12)$$

where $W_{N_r} = Re(\partial W / \partial N) / (\partial W / \partial \omega)$, $W_{N_i} = Im(\partial W / \partial N) / (\partial W / \partial \omega)$, and $W_p = (\partial W / \partial \rho_k) / (\partial W / \partial \omega)$. According to (8), the system described by (11) and (12) constitutes again a generalization of the well-known Lang and Kobayashi rate equations [15] used to study Fabry–Perot lasers operating in the presence of optical feedback. Through the generalized equations, both the static and dynamical behavior of every type of laser structure can be analyzed. The dynamic evolution of the carrier density is governed by the usual relation

$$\frac{dN}{dt} = \frac{I(t)}{e} - \frac{N(t)}{\tau_e} - GP(t) \quad (13)$$

where $N(t)$, τ_e , and $I(t)$ are the carrier density within the active zone, the carrier density lifetime, and the pump current, respectively. The optical gain G in the active region is linked to the carrier density through the relation

$$G(N) = \Gamma \frac{\partial g}{\partial N} (N - N_t) \quad (14)$$

where $\partial g / \partial N$ is the differential gain and N_t is the carrier density at the transparency (e.g., $G(N_t) = 0$). The confinement factor Γ takes into account the fraction of the optical power in the active region. According to (11) and (12), the change in the steady-state phase condition due to external optical feedback can be derived as follows:

$$\frac{1}{L} \int_{(L)} W_{N_i} \Delta N dz = -Im [W_p \gamma (1 - \rho_k^2)] \quad (15)$$

$$\Delta\omega = -\frac{1}{L} \int_{(L)} W_{N_r} \Delta N dz - Re [W_p \gamma (1 - \rho_k^2)] \quad (16)$$

By using the definition of W_{N_r} and W_{N_i} the effective phase-amplitude coupling coefficient α_{eff} is defined as the ratio [14]

$$\alpha_{\text{eff}} = -\frac{\int_{(L)} W_{N_r} \Delta N dz}{\int_{(L)} W_{N_i} \Delta N dz}. \quad (17)$$

By injecting (17) into (16), the variation of the angular frequency induced by external optical feedback can be rewritten following the relation

$$\Delta\omega = \frac{\alpha_{\text{eff}}}{L} \int_{(L)} W_{N_i} \Delta N dz - Re [W_p \gamma (1 - \rho_k^2)] \quad (18)$$

and from (15) to yield

$$\Delta\omega = \gamma (1 - \rho_k^2) (-\alpha_{\text{eff}} Im[W_p] - Re[W_p]). \quad (19)$$

Equation (19) gives the change in the lasing angular frequency when a semiconductor laser operates under optical feedback. As the parameter W_p is complex, it can be written as

$$W_p = |W_p| e^{-j\varphi} \quad (20)$$

where $|W_p|$ is the module and φ is the argument. According to (20), the angular frequency variation described by (19) can be written as follows:

$$\Delta\omega = -\gamma (1 - \rho_k^2) |W_p| (\alpha_{\text{eff}} Im[e^{-j\varphi}] + Re[e^{-j\varphi}]) \quad (21)$$

leading to

$$\Delta\omega \tau_i = -2C_k \gamma \sqrt{1 + \alpha_{\text{eff}}^2} \sin(\varphi + \arctan(\alpha_{\text{eff}})) \quad (22)$$

where τ_i the internal round-trip time and C_k is the coupling strength coefficient of the k -facet (assumed to be subjected to optical feedback) defined as

$$C_k = \frac{j\tau_i}{2} (1 - \rho_k^2) |W_p|. \quad (23)$$

Equation (23) constitutes a general expression of the coupling strength coefficient which takes into account the coupling between the k -facet to an external cavity. The coupling strength coefficient serves to quantify the sensitivity to external optical feedback of both the threshold gain and frequency variations [5], [15] of a semiconductor laser as well as to determine its coherence collapse threshold. But, above all, (23) shows the possibility of calculating the coupling strength coefficient of any type of laser structure. For instance, let us apply this general relation to a Fabry–Perot laser and to a straight-section DFB laser.

1) *Application to a Fabry–Perot Laser:* In what follows, the spatial hole burning effects are not taken into account. Under such a condition, it has been already shown that the Wronskian of a Fabry–Perot laser can be written following the relation [9], [14]

$$W = 2j\beta\rho_r(\rho_r\rho_l e^{-2j\beta L} - 1) \quad (24)$$

where $\rho_r\rho_l e^{-2j\beta L} - 1$ is the oscillation condition and β is the complex propagation constant which can be expressed as

$$\beta = nk_0 + j\frac{g - \alpha}{2} \quad (25)$$

where n is the refractive index, g is the optical gain, and α is the internal loss, all in the active region. After calculating W_p , it is easy to show that, by using (23) and (24), the coupling strength coefficient for a Fabry–Perot laser can be written as

$$C_k = \frac{1 - R_k}{2\sqrt{R_k}}, \quad \forall k = r, l \quad (26)$$

where $R_k = |\rho_k|^2$ is the reflectivity in intensity of the k -facet. Equation (26) coincides with the well-known value of the Fabry–Perot coupling strength coefficient published in [16].

2) *Application to a Uniform Grating DFB Laser:* It was shown that the Wronskian of a conventional DFB laser can be written as follows [5], [14]:

$$W = 4\beta_{\text{Bragg}} \frac{\sigma}{\kappa} \frac{F(\sigma L)}{\left(\tilde{\rho}_l - \frac{\tilde{X}}{j\kappa}\right) \left(\tilde{\rho}_r - \frac{X}{j\kappa}\right)} \quad (27)$$

where β_{Bragg} is the Bragg wavenumber, L is the length of the laser cavity, and κ is the coupling coefficient (e.g., internal feed-

back induced by the grating). In (27), $\tilde{\rho}_k$ is the complex amplitude reflectivity on the k -facet whose expression is given by $\tilde{\rho}_k = \rho_k e^{j\varphi_k}$ where ρ_k is the amplitude reflectivity of the k -facet and φ_k is the facet phase that describes the position of the facet in the corrugation. σ is the complex propagation constant such as $\sigma^2 = \kappa^2 + q^2$ where $q = \alpha_0 - j\delta_0$ with α_0 and δ_0 the laser losses and the Bragg deviation, respectively, both without optical feedback. The definition of the Bragg deviation (e.g., the detuning) δ_0 is given by the relation

$$\delta_0 = \beta - \beta_{\text{Bragg}} \quad (28)$$

where β is the emission wavenumber. In (27), the terms X and \hat{X} are defined by $X = \sigma + q$ and $\hat{X} = -\sigma + q$. Finally, the function $F(\sigma L)$ describing the threshold condition is expressed following the relation

$$F(\sigma L) = \left(1 - \tilde{\rho}_l \frac{\hat{X}}{j\kappa}\right) \left(1 - \tilde{\rho}_r \frac{\hat{X}}{j\kappa}\right) - \left(\tilde{\rho}_l - \frac{\hat{X}}{j\kappa}\right) \left(\tilde{\rho}_r - \frac{\hat{X}}{j\kappa}\right) e^{2\sigma L}. \quad (29)$$

Let us assume a straight-section DFB laser having an HR coating on the rear facet ($k = r$) and an AR coating on the emission facet ($k = l$). As the external optical feedback is assumed to be produced on the emission facet ($k = l$), let us only focus on the determination of the coefficient C_l . Thus, by using (23), (27), and (29), the coupling strength coefficient of such a structure can be written as

$$C_l = \frac{[(qL)^2 + (\kappa L)^2] [2\tilde{\rho}_r(qL)/\kappa L - j(1 + \tilde{\rho}_r^2)]}{qL[\kappa L(1 + \tilde{\rho}_r^2) - j\tilde{\rho}_r] + 2j\tilde{\rho}_r(qL)^2 - \kappa L}. \quad (30)$$

This relation is identical to that obtained by Favre [5] in his description of feedback effects in DFB lasers.

The above analytical expressions of C are obtained when the Wronskian can be expressed explicitly. For complex laser structures such as a chirped grating structure and for lasers exhibiting spatial hole burning above threshold, there are no known analytical solutions for the Wronskian. To cope with this difficulty, we propose to introduce a new method of calculations to determine the coupling strength factor for any kind of laser structure. The method can be applied above threshold and can take into account such effects as the spatial hole burning.

B. Numerical Implementation of the Method

By using (7), the amplitude of the reflection can be rewritten as

$$\gamma = \frac{\Delta\rho_k}{1 - \rho_k^2} e^{i\omega\tau} \quad (31)$$

where $\Delta\rho_k = \rho_{k,\text{eq}} - \rho_k$ is the overall variation of the reflectivity subjected to external optical feedback. Thus, by injecting (31) into (22), the variation of the lasing angular frequency can be written following the relation:

$$\Delta\omega\tau_i = -2C_k \frac{\Delta\rho_k}{1 - \rho_k^2} \sqrt{1 + \alpha_{\text{eff}}^2} h(\varphi) \quad (32)$$

where $h(\varphi) = e^{j\varphi} \sin(\varphi + \arctan(\alpha_{\text{eff}}))$, $h(\varphi)$ is a circular function such that $|h(\varphi)| \leq 1$. Equation (32) describes the interference condition between emitted and reflected fields lasing

at frequencies $\omega_0/2\pi$ and $\omega/2\pi$. Equation (32) serves to study the stability and the dynamic evolution of the system [17], [18] and clearly shows that, when $0 \leq \varphi \leq 2\pi$, every variation of the emission frequency can be explicitly calculated. More particularly, when $|h(\varphi)| = 1$, (32) reaches its maximum $(\Delta\omega\tau_i)_{\text{max}}$ and allows us to determine the coupling strength coefficient of the k -facet subjected to optical feedback through the relation

$$C_k = \frac{(\Delta\omega\tau_i)_{\text{max}}}{2\sqrt{1 + \alpha_{\text{eff}}^2}} \frac{1 - \rho_k^2}{\Delta\rho_k}. \quad (33)$$

According to (33), the calculation of the coupling strength coefficient is clearly obtained from the determination of the change in the lasing angular frequency $\Delta\omega$ introduced by the variation of the facet reflectivity. In Fig. 1, the algorithm used for the calculation of the coupling strength coefficient is outlined. At first, self-consistent calculations were made to predict the spectral behavior of the laser by using the transfer matrix method (TMM) [19]. In those simulations, variations of the effective index, of the confinement factor, and of the grating strength were taken into account. The spatial hole burning effect [10] was simulated by truncating the devices into small constant carrier density regions. The lasing conditions were then self-consistently found for any input current. In order to take into account the optical feedback, a variation of the facet reflectivity subjected to the external reflection is introduced by changing the facet reflectivity from ρ_k to $\rho_k + \delta\rho_k e^{j\theta}$. Under those conditions, the optical spectrum is recalculated as well as the new emission angular frequency ω for each value of θ such as $0 \leq \theta \leq 2\pi$. The knowledge of ω_0 and $\omega(\theta)$ allows us to determine explicitly the overall variation $\Delta\omega(\theta) = \omega(\theta) - \omega_0$. According to (33), the coupling strength coefficient C_k is given when $\Delta\omega(\theta)$ reaches its maximum value $(\Delta\omega)_{\text{max}}$.

C. Calculation of the Coherence Collapse Threshold

Due to the coupling strength coefficient, the onset of the coherence collapse regime occurring at a certain feedback level $\gamma = \gamma_C$ can be determined by using the well-known analytical relation [4]

$$\gamma_c = \frac{\omega_r^4 \tau_i^2}{16|C_k|^2 (1 + \alpha_{\text{eff}}^2) \omega_d^2}. \quad (34)$$

In (34), $\omega_r/2\pi$ is the relaxation frequency whereas $\omega_d/2\pi = 2\pi/K$ is the damping frequency. The damping K -factor is linked to the material structure and usually expressed as [20]

$$K = \frac{4\pi^2}{v_g} \left(\frac{\varepsilon_{NL}}{\partial g / \partial N} + \frac{1}{\alpha} \right) \quad (35)$$

where v_g is the group velocity and ε_{NL} is the nonlinear gain coefficient. In what follows, the K -factor is close to 0.5 ns, corresponding to a damping frequency of 12 GHz. It is important to stress that (34) holds under the assumption of weak optical feedback $\gamma_C < -30$ dB, $\alpha_{\text{eff}} > 1$, and $\omega_r \tau_i \gg 1$. It is also important to note that (34) is derived from an analysis based on the feedback loop theory where the laser and the feedback term are described by a general transfer function [4]. The theory leading to (34) can be applied to any laser provided that all the parameters appearing in (34) are properly defined through the gener-

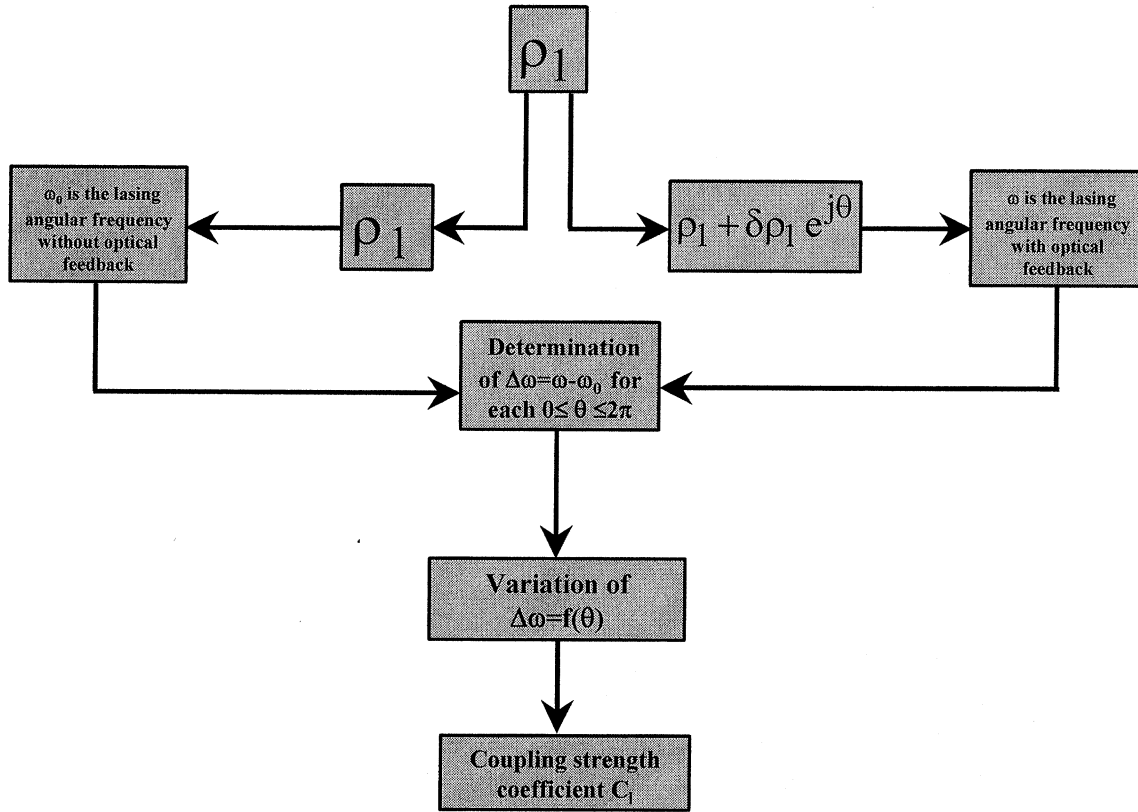


Fig. 1. Scheme of the algorithm used for the calculation of the coupling strength coefficient. The variation of the k -facet reflectivity subjected to the external reflection is done from ρ_k to $\rho_k + \delta\rho_k e^{j\theta}$. The knowledge of ω_0 and $\omega(\theta)$ allows us to determinate explicitly the overall variation $\Delta\omega(\theta) = \omega(\theta) - \omega_0$ as well as the coupling strength coefficient C_k through (15).

alized rate equation (8). The coherence collapse is a common name given to describe the dramatic spectral broadening occurring for a large range of feedback levels. Many papers describe the coherence collapse regime as coexisting chaotic attractors induced by the complicated irregular dynamics that occurs when the laser is operating above and not too close to threshold [21]. This regime can also be explained intuitively as an enhancement of the spontaneous emission occurring when the laser and the reflected fields are not correlated [22], [23]. Although the coherence collapse state is very detrimental to most applications, it has been shown that the induced spectral broadening may find useful applications. For instance, it has been utilized to stabilize a pump laser at a locked frequency by using a fiber Bragg grating [24].

By injecting (33) into (34), the coherence collapse threshold of the semiconductor laser can be expressed following the final relation

$$\gamma_{c,\text{dB}} = 10 \log \left(\frac{\omega_r^4 T_i^2}{4\omega_d^2} \left| \frac{\Delta\rho_k}{(\Delta\omega\tau_i)_{\max}(1 - \rho_k^2)} \right|^2 \right). \quad (36)$$

In the case of a DFB laser, it also appears from (34) that the coherence collapse threshold at a given output power P depends on facet phase effects via the complex coefficient C_k and the resonance frequency $\omega_r/2\pi$ whose expression is given by the relation $(\omega_r/2\pi) = A\sqrt{(P/\eta)(\varphi_r)}$ [25] where A and $\eta(\varphi_r)$ are a constant coefficient and the external efficiency (which depends on the facet phases), respectively. Such a dependence is taken into account in our numerical calculations.

In Section III, we propose to apply our proposed coupling strength coefficient method to conventional AR/HR DFB lasers. These simulations will be compared to (30), which matches the results of [5]. In Section IV, the method will be applied to chirped grating DFB lasers, and a comparison of the predicted coherence collapse threshold will be made through experiments.

III. APPLICATION TO AR/HR UNIFORM GRATING DFB LASERS

In this paragraph, the method which has been described in Section II is numerically applied to AR/HR DFB lasers such as that depicted in Fig. 2. Let us assume that the external optical reflection is produced on the AR-coated left facet while the rear facet on the right has an HR coating. The amplitude reflectivity of the laser is assumed to be $\tilde{\rho}_r = 0.97e^{j\varphi_r}$ for the HR facet and $\tilde{\rho}_l = 0.00e^{j\varphi_l}$ for the AR-coated facet. Due to the AR coating, the optical field depends only on the HR facet phase φ_r . In order to check the method proposed in the previous section, we first calculate the coupling strength coefficients by using the analytical method described in [5]. In Fig. 3, the variation of the coupling strength coefficient C_l versus the normalized grating coupling coefficient κL derived from (30) is reported for two different facet phase cases $\varphi_r = \pi$ and $\varphi_r = \pi/2$. The normalized grating coupling coefficient κL is in the range from 0.30 to 0.90. A decrease of the coefficient C_l when the normalized grating coupling coefficient increases is observed as expected in [5]. The previous values reported in Fig. 3 can be recalculated by using the numerical method based on the laser an-

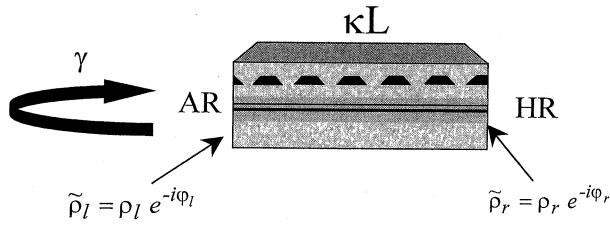


Fig. 2. Design of the AR/HR straight-section studied laser. The amount γ denotes the optical feedback reinjected into the cavity through the left facet and κL is the normalized coupling coefficient. $\tilde{\rho}_l$ and $\tilde{\rho}_r$ correspond to the complex amplitude reflectivities on the AR and HR facets, respectively.

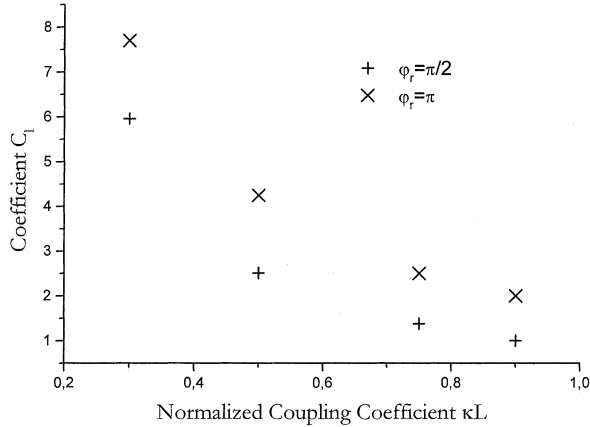


Fig. 3. Variations of the calculated coupling strength coefficient versus the normalized grating coupling coefficient ($0.3 \leq \kappa L \leq 0.9$) for a 350- μm AR/HR conventional DFB laser. The phase of the HR facet φ_r is fixed either to $\pi/2$ (+ points) or π (x points).

gular frequency variation. The emission angular frequency ω_0 without optical feedback ($\gamma = 0$) is first calculated for each value of κL . Then, let us assume that an external reflection on the left facet induces a variation of the reflectivity from ρ_l to $\rho_l + \delta\rho_l e^{i\theta}$. In the calculations, the external optical feedback is chosen such that $\gamma^2 = 2 \cdot 10^{-4}$. By varying the phase θ from 0 to 2π , the new emission angular frequency ω in the presence of optical feedback is calculated. In Fig. 4, the overall variation $\Delta\omega\tau_i(\theta) = (\omega(\theta) - \omega_0)\tau_i$ is reported for each value of κL . In the simulations, the laser cavity length is kept to 350 μm and corresponds to an internal round-trip time of $\tau_i = 7.5$ ps. Each point is obtained for a given feedback phase θ and a fit is then added for visual help. According to the theory, the response to optical feedback from the front facet is sinusoidal. Taking into account the AR coating, the coupling strength coefficient on the left facet described by (33) can be simply written and calculated following the relation:

$$C_l = \frac{(\Delta\omega\tau_i)_{\max}}{2\Delta\rho_l \sqrt{1 + \alpha_{\text{eff}}^2}} \quad (37)$$

where $|\Delta\rho_l|^2 = \gamma^2$ [see (7)]. In the simulations, the linewidth enhancement factor α_H is chosen to be equal to 3.00. In Fig. 5, a comparison among the coupling strength coefficients C_l calculated either with the analytical method (+ symbol) or with the method of the angular frequency variation (x symbol) is shown. In Fig. 5(a), the facet phase on the right facet is $\varphi_r = \pi$ while it is assumed to be equal to $\varphi_r = \pi/2$ in Fig. 5(b). Both figures show that the coupling strength coefficients calculated from

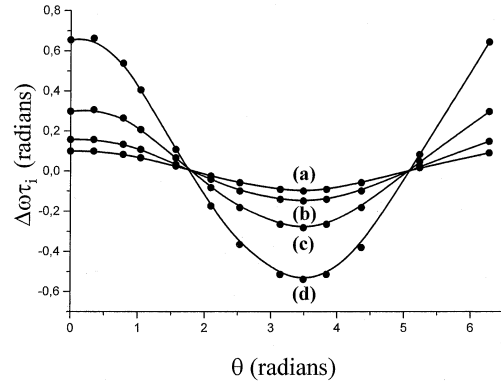


Fig. 4. Variations of the calculated normalized laser angular frequency $\Delta\omega\tau_i$ versus the phase θ for a 350- μm AR/HR conventional DFB laser and for different normalized grating coupling coefficients κL : (a) $\kappa L = 0.3$, (b) $\kappa L = 0.5$, (c) $\kappa L = 0.7$, and (d) $\kappa L = 0.9$.

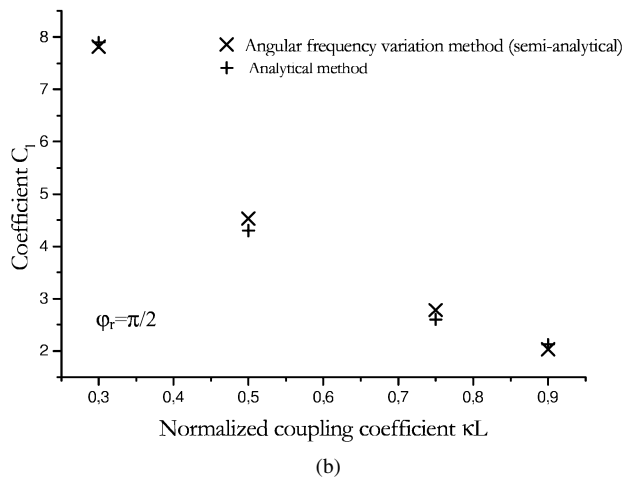
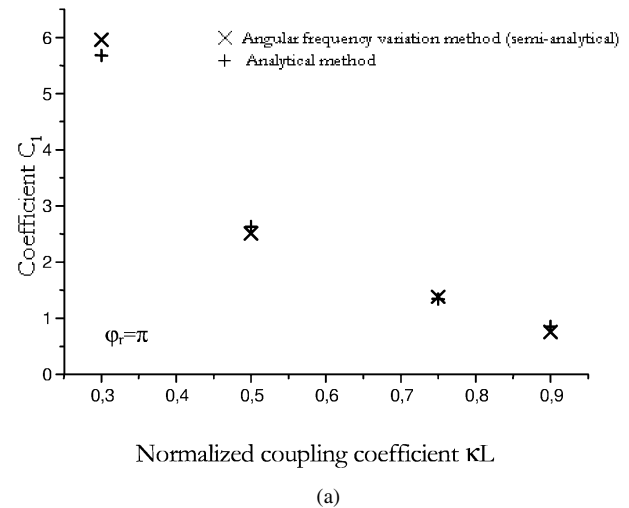


Fig. 5. Variations of the coupling strength coefficients C_l versus the normalized grating coupling coefficient calculated either with the analytical method (+ points) or with the method of the angular frequency variation (x points). The laser is a 350- μm AR/HR conventional DFB. Two facet phase cases φ_r are investigated: (a) $\varphi_r = \pi$ and (b) $\varphi_r = \pi/2$.

(37) are the same as those calculated by using (30). These comparative results demonstrate that both methods can be equivalently used for calculating the coupling strength coefficient. In the next paragraph, we propose to apply the method of the angular frequency variation to the case of chirped grating DFB

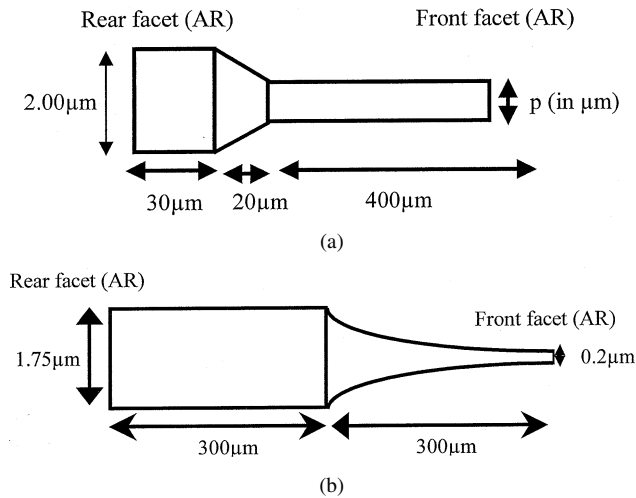


Fig. 6. Designs of the chirped-grating DFB lasers investigated with their different marks. They are made of a straight section followed by a varying width stripe section and have an AR coating on both facets so as to suppress facet phase effects. Design (a): the tip width p is in the range from 1.1 to 1.7 μm . Design (b): the grating coupling coefficient is in the range from 10 to 100 cm^{-1} .

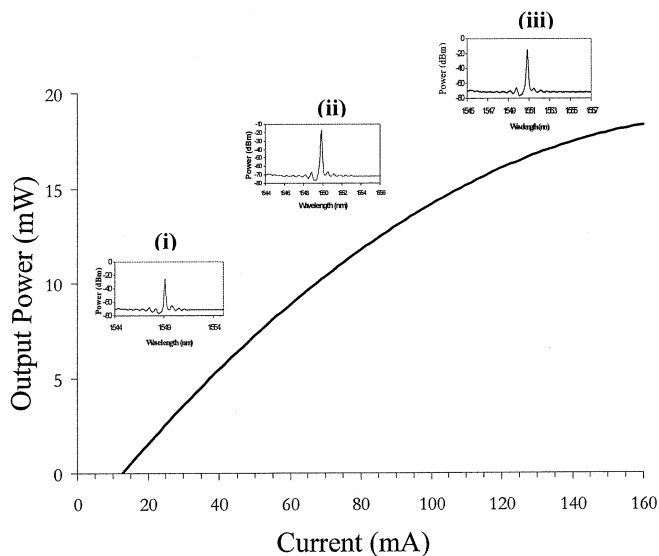


Fig. 7. Light-current characteristic relative to design (a) in Fig. 6. Threshold current at 25 $^{\circ}\text{C}$: $I_{\text{th}} = 12$ mA, External efficiency at 25 $^{\circ}\text{C}$: $\eta = 0.19$ W/A. Experimental optical spectra recorded at 3 mW (i), 6 mW (ii), and 15 mW (iii) are reported in the inset.

laser structures. The coupling strength coefficients as well as the coherence collapse thresholds of two different designs are compared to each other as well as to experimental results.

IV. CHIRPED-GRATING DFB LASERS

A. Description of Chirped-Grating DFB Structures

It has been shown in the previous section that AR/HR devices suffer from dispersion from laser to laser [7]. Indeed, due to interference effects between the grating and the facets, the lasing properties are highly dependent on cleavage plane variations as small as a fraction of a wavelength. To clear the fabrication process from such dependence, AR coatings on both facets can be used when combined to an appropriate structure

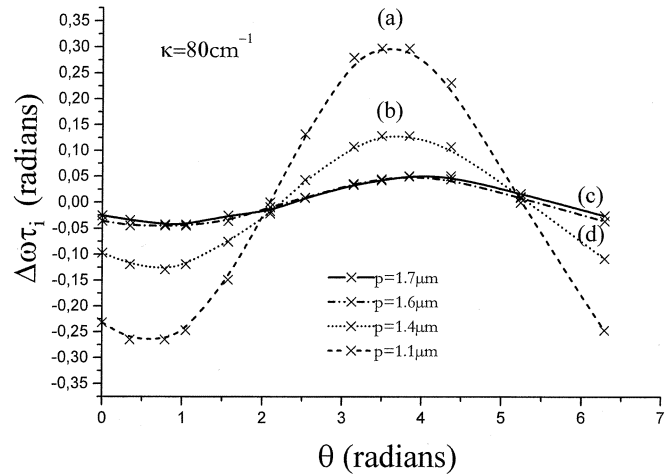


Fig. 8. Variations of the calculated normalized laser angular frequency $\Delta\omega\tau_i$ versus the phase θ for design (a). The grating coupling coefficient is equal to 80 cm^{-1} . Simulations are conducted for the following values of the parameter p : (a) $p = 1.1$ μm , (b) $p = 1.4$ μm , (c) $p = 1.6$ μm , and (d) $p = 1.7$ μm .

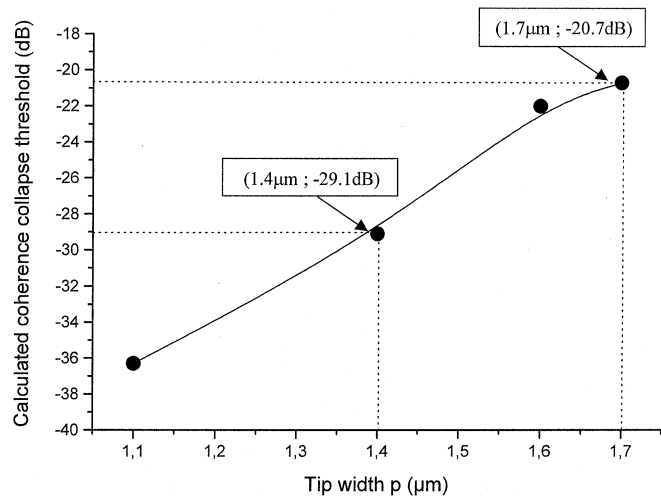


Fig. 9. Variations of the calculated coherence collapse threshold versus the tip width for design (a). Each point corresponds to a calculated value whereas a fit has been added to improve clarity.

such as a phase-shift laser [26]. However, in most cases, a high fabrication accuracy is needed to control the laser spectral characteristics and the production of such structures remains a technological challenge. Another way to clear the problem is to use chirped-grating DFB lasers which are based on a stripe engineering approach [27], [28]. The two designs of Fig. 6(a) and (b) will be investigated in this paper. The lasers can be divided into a straight section (left) followed by a varying-width stripe section (right). The lasers have an AR coating on both facets so as to suppress facet phase effects. A uniform grating is built using conventional holographic techniques. However, its optical pitch varies along the device due to the dependence of the effective index with the stripe width. The variation of the effective index in the device is designed such as to break the symmetry of a uniform grating laser and to allow for a proper spectral selection. Due to those structures, single-mode operations have been achieved and already reported elsewhere [8], [29], [30]. As an example, the light current characteristic $L(I)$ corresponding to

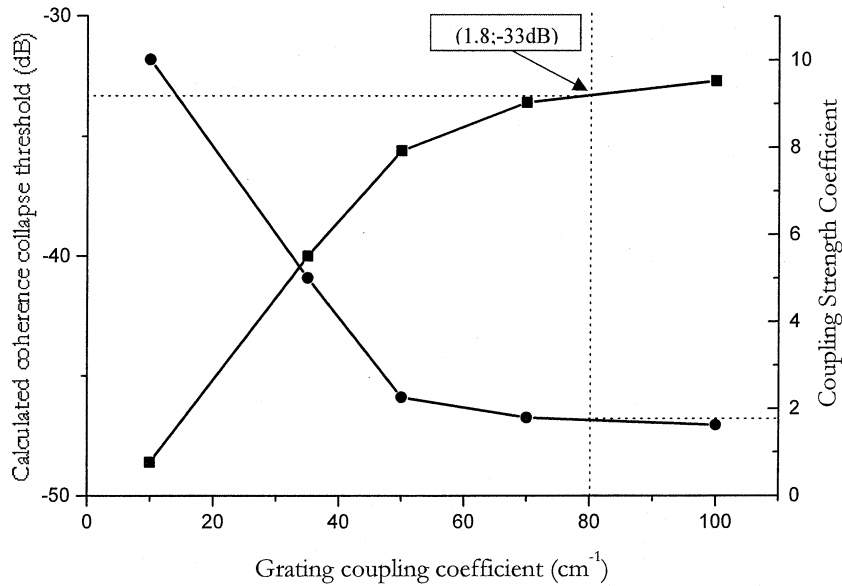


Fig. 10. Variations of the coupling strength coefficients (black dots) and of the coherence collapse threshold (black squares) versus the grating coupling coefficient for design (b).

design (a) is shown in Fig. 7 together with the experimental optical spectra recorded at 3 mW (i), 6 mW (ii), and 15 mW (iii). Low threshold currents of 12 mA combined with an external facet efficiency of 0.19 W/A are obtained. No deleterious effect from the spatial hole burning is observed, neither kinks nor spectral variations, even under high injected current.

B. Calculation of the Coherence Collapse Threshold

In the calculations, the design parameters are the width of the tip p (i.e., the width of the end of the varying width stripe section on the emission facet) which varies from 1.0 to 1.7 μm for design (a). The straight section has a grating coupling coefficient κ of 80 cm^{-1} . The grating coupling coefficient varies from 10 to 100 cm^{-1} for design (b). The tip width is $0.2\text{ }\mu\text{m}$. Due to the variation of the effective index and of the confinement factor, both the grating coupling coefficient and the Bragg wavelength are dependent on stripe width. As a consequence, the determination of the coupling strength coefficients cannot be realized with the analytical method described in [5] [see (30)]. These calculations have therefore been realized with the method of the angular frequency variation. The reflection is assumed to be produced on the emission facet (right facet) for all designs. For the simulations, the linewidth enhancement factor is $\alpha_H = 3.0$ whereas optical feedback is again equal to $\gamma^2 = 2 \cdot 10^{-4}\text{ GHz}$. The resonance $\omega_r/2\pi$ and damping $\omega_d/2\pi$ frequencies are 8 and 12 GHz, respectively. In Fig. 8, the angular frequency variation ($\Delta\omega\tau_i$) induced by optical feedback is plotted for design (a) versus the feedback phase θ for different values of the tip width. As predicted, a sinusoidal behavior is obtained whose maxima serve again to calculate the coupling strength coefficient of the right facet C_r , as well as the coherence collapse threshold. In Fig. 9, the calculated coherence collapse threshold variation is reported versus the tip width p . Each point corresponds to a calculated value whereas a fit has been added for improved clarity. As it is clearly shown, the resistance to op-

tical feedback decreases with the tip width. We explain this effect by the reduced average coupling coefficient since κ decreases with the stripe width. Now, let us consider design (b) whose tip width is $0.2\text{ }\mu\text{m}$ (cf. Fig. 6). The laser parameters are $\alpha_H = 3.5$, $\omega_r/2\pi = 8\text{ GHz}$ and $\omega_d/2\pi = 12\text{ GHz}$ for the linewidth enhancement factor, the resonance frequency, and the damping frequency, respectively. The coupling grating coefficient is now a parameter in the range from 10 to 100 cm^{-1} . In Fig. 10, variations of coupling strength coefficients (black dots) and of coherence collapse threshold (black squares) are reported. As predicted by theory, the sensitivity to optical feedback decreases when a higher grating coupling coefficient is used. In the calculations, the coupling strength coefficient is in the range from 2 to 10 while the coherence collapse threshold varies from -48 to -32 dB . In the case of $\kappa = 80\text{ cm}^{-1}$, the calculated coupling strength coefficient C_r is equal to 1.8, leading to a coherence collapse threshold of -33 dB .

C. Comparison With Measurements

The lasers used for the experimental work are buried ridge stripes (BRS) with proton implantation whose vertical structure has already been published in detail [31]. Design (a) (with $p = 1.4\text{ }\mu\text{m}$ and $p = 1.7\text{ }\mu\text{m}$) and design (b) ($\kappa = 80\text{ cm}^{-1}$) have been fabricated and tested. In order to avoid undesirable reflections, an AR coating in the range of 10^{-4} was applied on each facet. The onset of the coherence collapse is determined when a drastic broadening of the emission line occurs (at $\pm 1\text{ dB}$) with respect to the return loss (RL) level. An optical spectrum analyzer having a resolution of 10 pm was used for this purpose. Two lasers have been measured for each design with similar results. Taking into account the coupling loss coefficient η from the laser into the fiber which was optically measured to be equal to 3 dB, the coherence collapse threshold can be derived from the critical return loss level RL_c according to the relation

$$\gamma_c = \text{RL}_c + 2\eta_{\text{dB}} \quad (38)$$

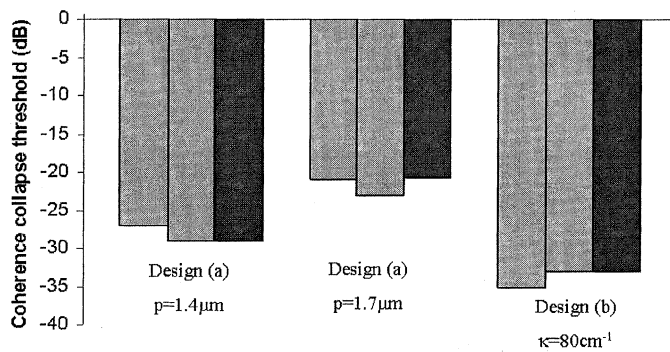


Fig. 11. Comparison between measured (in gray) and calculated (in black) coherence collapse thresholds γ_C . Design (a): $p = 1.4 \mu\text{m}$, $\gamma_C = -28$ dB (for a prediction of -29.1 dB). Design (a): $p = 1.7 \mu\text{m}$, $\gamma_C = -22$ dB (for a prediction of -20.7 dB). Design (b): $\gamma_C = -34$ dB (for a prediction of -33 dB).

where the factor 2 is due to the round trip in the external cavity. In all cases, the injected power was fixed to 10 mW leading to a resonance frequency of $\omega_r/2\pi = 8$ GHz whereas the damping frequency was measured to be equal to $\omega_d/2\pi = 12$ GHz. By using the experimental method described in [32], the effective linewidth enhancement factor was also measured to be equal to 3.0 [for design (a)] and 3.5 [for design (b)].

In Fig. 11, a comparison of the simulation results with the measured coherence collapse threshold (in gray) for both design (a) (tip width $p = 1.4 \mu\text{m}$ and $p = 1.7 \mu\text{m}$) and (b) ($\kappa = 80 \text{ cm}^{-1}$) are reported. Two lasers have been experimentally investigated for each configuration under study. Thus, for a tip width of $1.4 \mu\text{m}$ [design (a)], the average coherence collapse threshold is -28 dB for -29.1 dB predicted. In the case of a tip width of $1.7 \mu\text{m}$, the average critical return loss increases leading to a measured coherence collapse threshold of -22 dB for -20.7 dB predicted. Concerning design (b), the average coherence collapse threshold is -34 dB for -33 dB predicted. For all designs, a very good agreement between calculations and measurements is clearly obtained. In conclusion, based on the lasing angular frequency variation induced by optical feedback, the prediction of the feedback sensitivity via the coupling strength coefficient and then of the coherence collapse threshold of all laser structures is demonstrated.

It is important to point out that this general method of calculation does not make use of the knowledge of the Bragg wavelength and can be used at and above threshold. Finally, even though this has not been studied in this paper, it is important to highlight that this method can be used experimentally to measure the coupling strength coefficient of a semiconductor provided the feedback phase θ as well as the feedback level γ are properly controlled.

V. CONCLUSION

The use of Green's functions theory has led to a generalization of the well-known Lang and Kobayashi equations. These generalized rate equations can be applied to any type of laser cavity and allow us to derive a very general expression of the coupling strength coefficients. This expression shows that the variation of the lasing angular frequency can always be

expressed using a circular function when written with respect to the feedback phase. More importantly, the knowledge (or measurement) of this function suffices to predict the laser sensitivity to optical feedback. As a main consequence of our approach, the laser feedback sensitivity can be evaluated at a very early stage of the design optimization of complex laser structures. The newly proposed approach has first been applied to Fabry–Perot and uniform DFB lasers with AR/HR coatings. Identical results compared to previous publications have been found, demonstrating the validity of the new approach. More importantly, the sensitivity to optical feedback of chirped grating DFB lasers that could not be described by previous theories has been investigated. Excellent qualitative and quantitative agreement between the theory and our experimental measurements in terms of coherence collapse threshold has been obtained on all the designs under study.

In summary, we have demonstrated new and powerful tools for calculating the coherence collapse threshold of any laser structures. These results are of prime importance to evaluate the sensitivity to external optical feedback of semiconductor lasers and to predict their dynamical behavior in transmission. They apply even in the case of strong spatial hole burning and may also lead to the experimental measurement of the coupling strength coefficients of semiconductor lasers.

REFERENCES

- [1] D. Lenstra, B. H. Verbeek, and A. J. Den Boef, "Coherence collapse in single-mode semiconductor lasers due to optical feedback," *IEEE J. Quantum Electron.*, vol. QE-21, pp. 674–679, June 1985.
- [2] R. B. Clarke, "The effect of reflections on the system performances of intensity modulated laser diodes," *J. Lightwave Technol.*, vol. 9, pp. 741–749, June 1991.
- [3] F. Grillot, B. Thedrez, F. Mallecot, Ch. Chaumont, S. Hubert, M. F. Martineau, A. Pinquier, and L. Roux, "2.5 Gbit/s transmission characteristics of $1.3 \mu\text{m}$ DFB lasers with external optical feedback," *IEEE Photon. Technol. Lett.*, vol. 14, pp. 101–103, Jan. 2002.
- [4] J. Helms and K. Petermann, "A simple analytic expression for the stable operation range of laser diodes with optical feedback," *IEEE J. Quantum Electron.*, vol. 26, pp. 833–836, May 1990.
- [5] F. Favre, "Theoretical analysis of external optical feedback on DFB semiconductor laser," *IEEE J. Quantum Electron.*, vol. QE-23, pp. 81–88, Jan. 1987.
- [6] O. Nilsson and J. Buus, "Linewidth and feedback sensitivity of semiconductor diode lasers," *IEEE J. Quantum Electron.*, vol. 26, pp. 2039–2042, Dec. 1990.
- [7] F. Grillot, B. Thedrez, O. Gauthier-Lafaye, M. F. Martineau, V. Voiriot, J. L. Lafrayette, J. L. Gentner, and L. Silvestre, "Coherence collapse threshold of $1.3 \mu\text{m}$ semiconductor DFB lasers," *IEEE Photon. Technol. Lett.*, vol. 15, pp. 9–11, Jan. 2003.
- [8] F. Grillot, B. Thedrez, F. Mallecot, C. Chaumont, S. Hubert, M. F. Martineau, A. Pinquier, and L. Roux, "Analysis, fabrication and characterization of $1.55 \mu\text{m}$ selection-free tapered stripe DFB lasers," *IEEE Photon. Technol. Lett.*, vol. 14, pp. 1040–1042, Aug. 2002.
- [9] C. H. Henry, "Theory of spontaneous emission noise in open resonators and its application to lasers and optical amplifiers," *J. Lightwave Technol.*, vol. LT-4, pp. 288–297, Mar. 1986.
- [10] W. S. Rabinovich and B. J. Feldman, "Spatial hole burning effects in distributed feedback lasers," *IEEE J. Quantum Electron.*, vol. 25, pp. 20–29, Jan. 1989.
- [11] K. Ujihara, "Phase noise in a laser with output coupling," *IEEE J. Quantum Electron.*, vol. QE-20, pp. 814–818, July 1984.
- [12] G. H. Duan, P. Gallion, and G. Debarge, "Analysis of the phase-amplitude coupling factor and spectral linewidth of distributed feedback and composite-cavity semiconductor lasers," *IEEE J. Quantum Electron.*, vol. QE-26, pp. 32–43, Jan. 1990.
- [13] B. Tromborg, H. Olesen, and X. Pan, "Theory of linewidth for multi-electrode laser diodes with spatially distributed noise sources," *IEEE J. Quantum Electron.*, vol. 27, pp. 178–192, Feb. 1991.

- [14] G. H. Duan, P. Gallion, and G. P. Agrawal, "Dynamic and noise properties of tunable multielectrode semiconductor lasers including spatial hole burning and nonlinear gain," *IEEE J. Quantum Electron.*, vol. QE-29, pp. 844–855, Mar. 1993.
- [15] R. Lang and K. Kobayashi, "External optical feedback effects on semiconductor injection laser properties," *IEEE J. Quantum Electron.*, vol. QE-16, pp. 347–355, Mar. 1980.
- [16] K. Petermann, "External optical feedback phenomena in semiconductor lasers," *IEEE J. Select. Topics Quantum Electron.*, vol. 1, pp. 480–488, Mar./Apr. 1995.
- [17] H. Olesen, J. H. Osmunden, and B. Tromborg, "Nonlinear dynamics and spectral behavior for an external cavity laser," *IEEE J. Quantum Electron.*, vol. QE-22, pp. 762–773, June 1986.
- [18] B. Tromborg, J. H. Osmunden, and H. Olesen, "Stability analysis for a semiconductor laser in an external cavity," *IEEE J. Quantum Electron.*, vol. QE-20, pp. 1023–1032, Sept., 1984.
- [19] G. Björk and O. Nilsson, "A new exact and efficient numerical matrix theory of complicated laser structures: Properties of asymmetric phase-shifted DFB lasers," *J. Lightwave Technol.*, vol. LT-5, pp. 140–146, Jan. 1987.
- [20] K. Uomi, M. Aloki, T. Tsuchiya, and N. Chimone, "Dependence of relaxation oscillation frequency and damping K factor on the number of quantum wells in 1.55 μm InGaAsP DFB lasers," *IEEE Photon. Technol. Lett.*, vol. 3, pp. 493–495, June 1991.
- [21] J. Mork, B. Tromborg, and J. Mark, "Chaos in semiconductor lasers with optical feedback: Theory and experiment," *IEEE J. Quantum Electron.*, vol. 28, pp. 93–108, Nov. 1992.
- [22] J. Mork, B. Tromborg, and P. L. Christiansen, "Bistability and low-frequency fluctuations in semiconductor lasers with optical feedback: A theoretical analysis," *IEEE J. Quantum Electron.*, vol. 24, pp. 123–133, Feb. 1988.
- [23] B. Tromborg and J. Mork, "Non-linear injection locking dynamics and the onset of coherence collapse in external cavity lasers," *IEEE J. Quantum Electron.*, vol. 26, pp. 642–654, Apr. 1990.
- [24] A. Ferrari, G. Ghisloti, S. Balsamo, and G. Troiano, "Wavelength-locking and coherence collapsed calculation of multimode semiconductor lasers induced by external injection," *IEEE Photon. Technol. Lett.*, vol. 15, pp. 1041–1043, Aug. 2003.
- [25] R. S. Tucker and I. P. Kaminow, "High frequency characteristics of directly modulated InGaAsP ridge waveguide and buried heterostructure lasers," *J. Lightwave Technol.*, vol. LT-2, pp. 385–393, Aug. 1984.
- [26] H. A. Haus and C. V. Shank, "Antisymmetric taper of distributed feedback lasers," *IEEE J. Quantum Electron.*, vol. QE-12, pp. 532–539, Sept. 1976.
- [27] G. P. Agrawal and A. H. Bobeck, "Modeling of distributed feedback semiconductor lasers with axially-varying parameters," *IEEE J. Quantum Electron.*, vol. 24, Dec. 1988.
- [28] J. Hong, W. P. Huang, T. Makino, and G. Pakulski, "Static and dynamic characteristics of MQW DFB lasers with varying ridge width," in *Proc. Inst. Elect. Eng.*, vol. 141, 1994.
- [29] F. Mallécot, F. Grillot, B. Thédrez, Ch. Chaumont, S. Hubert, M. F. Martineau, A. Pinquier, J. Py, and L. Roux, "Selection-free WDM DFB lasers for STM16 applications," in *Proc. OFC*, Anaheim, CA, Mar. 17–22, 2002, WF7, pp. 212–213.
- [30] B. Thédrez, V. Voiriot, S. Hubert, J. L. Lafrayette, L. Roux, F. Grillot, J. L. Gentner, and B. Fernier, "New WDM DFB structure for facet phase-free uniform performances," *Proc. ISCL*, Sept. 25–28, 2000.
- [31] Ph. Pagnod-Rossiaux, F. Gaborit, N. Tschertner, L. Roux, C. Stark, and B. Fernier, "High temperature (Ga)InAsP/high band gap GaInAsP barriers 1.3 μm SL-MQW lasers grown by gas source MBE," *J. Cryst. Growth*, vol. 175/176, pp. 948–954, 1996.
- [32] R. Schimpe, J. E. Bowers, and T. L. Koch, "Characterization of frequency response of 1.5 μm InGaAsP DFB laser diode and InGaAs PIN photodiode by heterodyne measurement technique," *Electron. Lett.*, vol. 22, no. 9, pp. 453–454, 1986.



Frédéric Grillot (M'02) was born in Versailles, France, on August 22, 1974. He received the M.Sc. degree in physics on light-matter interaction from the University of Dijon, Dijon, France, in 1999 and the Ph.D. degree in electrical engineering from the University of Besançon, Besançon, France, in 2003.

His doctoral research activities were conducted within Opto+, Alcatel Research & Innovation Center, Marcoussis, France. Along with his Ph.D. work, he has designed and conceived monomode DFB lasers exhibiting a strong resistance to external optical feedback for 2.5 Gb/s isolator-free transmissions. His work has thus led to understand both quantitatively and qualitatively the effects induced by optical feedback on the lasers and to relate these effects to the degradations in the bit-error-rate plots. Successful and state-of-the art 2.5-GB/s 85 °C transmissions without floor and with low penalties have been achieved open the way for all-optical telecommunication networks. Since June 2003, he has been with the Institut d'Electronique Fondamentale, University of Paris-Sud, Paris, France, through a Postdoctoral position supported by both Alcatel Research and Innovation and the Centre National de la Recherche Scientifique (CNRS). His main research activities are now on polarization-independent waveguides for telecommunication wavelengths and integrated optics modeling.

Dr. Grillot is a Member of la Société Française d'Optique.

Bruno Thédrez was born in Saint-Nazaire, France, in 1960. He received the master degree from Ecole Supérieure d'Electricité, Gif/Yvette, France, in 1984 and the Ph.D. degree from Ecole Nationale Supérieure des Télécommunications, Paris, France, in 1988.

From 1989 to 1993, he was involved with AlGaAs semiconductor lasers for short-pulse generation at the University of Maryland, College Park. In 1994, he was with the University of Tokyo, Tokyo, Japan, where he was engaged in short-pulse compression schemes based on semiconductor laser sources. He moved to the Centre National de la Recherche Scientifique (CNRS), Orsay, France, in 1995 and joined the Corporate Research Center of Alcatel in 1996 where his work concentrated on the design and fabrication of 1.55- μm DFB lasers. From October 2000 to present, he has been head of a research group devoted to the fabrication of directly modulated lasers for optical telecommunication. Since December 2002, his group field of competency extended to optical regeneration and optical amplification.



Guang-Hua Duan (S'88–M'90–SM'01) was born in Hubei Province, China, on January 23, 1964. He received the B.E. degree from Xidian University, Xi'an, China, in 1983 and the M.E. and Ph.D. degrees both from the Ecole Nationale Supérieure des Télécommunications (ENST), Paris, France, in 1987 and 1991, respectively, all in applied physics.

He was habilitated to direct researches by Université de Paris-Sud in 1995. From 1983 to 1985, he was engaged in research on optical fiber measurements at the Guilin Institute of Optical Communications, Guilin, China. From 1991 to 1992, he was a Post-Doctoral Fellow supported by both Alcatel Alsthom Research and ENST. From 1992 to 2000, he was an Assistant and then an Associate Professor with ENST. From 1998 to 1999, he was with the University of Maryland, College Park, as a Visiting Associate Professor. He joined Opto+, Alcatel Research and Innovation Center, Marcoussis, France, in October 2000. He is now a Member of the Alcatel Technical Academy, with research activities on photonic crystals, advanced semiconductor lasers and functional optoelectronic subsystems for core and metro networks. He is the author or coauthor of more than 100 research papers, eight patents, and a contributor to the book *Semiconductor Lasers: Past, Present, and Future* (AIP Press, 1995). He lectures in the fields of electromagnetism, optoelectronics and laser physics in ENST and in Ecole Supérieure d'optique.

Dr. Duan is a Member of la Société Française d'Optique.